Clays and Clay Minerals, Vol. 56, No. 6, 633–644, 2008.

THE STANDARD GIBBS ENERGY OF FORMATION OF Fe(II)Fe(III) HYDROXIDE SULFATE GREEN RUST

KARINA BARBARA AYALA-LUIS*, CHRISTIAN BENDER KOCH, AND HANS CHRISTIAN BRUUN HANSEN

Department of Basic Sciences and Environment, Faculty of Life Sciences, University of Copenhagen, Thorvaldsensvej 40, DK-1871, Frederiksberg C., Denmark

Abstract—Mixed $Fe^{II}Fe^{III}$ hydroxides, commonly referred to as 'green rusts' (GRs), are important reactive phases in both man-made and natural geochemical systems. Determinations of the standard Gibbs energy of formation of GRs are needed to understand and predict the occurrence and possible reactions of GRs in these systems. Slow acid titration of crystalline green rust sulfate (GR_{SO_4}) with the formation of magnetite was used as a novel method to determine the standard Gibbs energy of formation of GR_{SO_4}, $\Delta_f G^o(GR_{SO_4})$. Aqueous suspensions of GR_{SO_4}, with pH slightly >8, were titrated slowly with 1 M H_2SO_4 until pH = 3 under strict anoxic conditions. Powder X-ray diffraction and Mössbauer analysis revealed that magnetite was the only solid phase formed during the initial part of the titration, where the equilibrium pH was maintained above 7.0. The ratio of Fe^{2+} release to consumption of protons confirmed the stoichiometry of dissolution of GR_{SO_4} and the formation of magnetite at equilibrium conditions. The estimate of the absolute value of $\Delta_f G^o(GR_{SO_4})$ was -3819.43 ± 6.44 kJ mol^{-1} + $y \times [\Delta_f G^o(H_2O_{(l)})]$, where y is the number of interlayer water molecules per formula unit. The logarithm of the solubility product, log K_{sp}, was estimated to be -139.2 ± 4.8 and is invariable with y. Using the new value for $\Delta_f G^o(GR_{SO_4})$, the reduction potentials of several GR_{SO_4}-Fe oxide couples were evaluated, with the GR_{SO_4}-magnetite half cell showing the smallest redox potential at pH 7 and free ion activities of 10^{-3}.

Key Words—Acid Titration, Gibbs Energy of Formation, Green Rust, Layered Double Hydroxides, Magnetite, Mössbauer Spectroscopy, Solubility Product.

INTRODUCTION

Fe oxides/hydroxides are environmentally significant solid phases which influence the geochemistry of many important substances such as nutrients, heavy metals, and organic pollutants (Cornell and Schwertmann, 2003). Fe^{II}-Fe^{III} hydroxide salts, so called 'green rusts' (GRs), represent one branch of the Fe oxides/hydroxides family and, as partly reduced intermediates, are thought to play an important role in the iron cycle (Bernal *et al*., 1959; Genin *et al*., 2006).

Green rusts have the general formula $[Fe^{II}_{(1-x)}Fe^{III}_x(OH)_2]^{x+}[(x/n)A^{n-}\cdot yH_2O]^{x-}$, where, x is the ratio $Fe^{III}/(Fe^{III}+Fe^{II})$, A is an n-valent anion, and y is the number of intercalated water molecules per formula unit. This general formula is characteristic of the materials known as 'layered double hydroxides' or LDHs. The structure of GR consists of positively charged brucite-like layers, where the metal ions are octahedrally coordinated to hydroxyl groups, alternating with negatively charged interlayers composed of water and charge-compensating anions, *e.g.* CO_3^{2-}, SO_4^{2-}, and Cl^- (designated GR_{ANION}). In the laboratory, GR can be synthesized using different methods. Commonly used methods comprise controlled chemical or electrochemical oxidation of zero-valent iron, partial oxidation of a ferrous solution, or coprecipitation from mixed Fe^{II}-Fe^{III} solutions (Hansen, 2001).

In nature, GRs are known to occur in hydromorphic soils, where the dissolution/precipitation reactions of GRs may control the solution concentrations of Fe^{II} (Bourrie *et al*., 1999). They are also formed as intermediary or end-products in the corrosion processes of Fe^0 in permeable reactive barriers, and of steel in marine environments (Furukawa *et al*., 2002; Phillips *et al*., 2003; Rodriguez and Gonzalez, 2006). Due to their strong reducing capacity, GRs participate in redox reactions with: (1) oxyanions such as CrO_4^{2-} and SeO_4^{2-}; (2) radionuclides such as U^{VI}; (3) organic pollutants, *e.g.* halogenated aliphatics and nitroaromatic compounds including certain pesticides; and (4) other reducible compounds, *e.g.* nitrate and nitrite (Hansen *et al*., 1994, 1996; Legrand *et al*., 2004; Myneni *et al*., 1997).

Accurate prediction of the geochemical processes involving GRs requires that the standard Gibbs energy of formation, $\Delta_f G^o$, of GR be known with sufficient certainty. Among the different methods to determine $\Delta_f G^o$, solubility measurements are widely used. However, the solubility product of GR cannot be determined directly (reaction 1) due to the extremely low solubility of Fe^{3+}. Therefore, Hansen *et al*. (1994) determined $\Delta_f G^o(GR_{SO_4})$ indirectly as

* E-mail address of corresponding author:
kayala@life.ku.dk
DOI: 10.1346/CCMN.2008.0560604

-3668.7 ± 4 kJ mol^{-1} for the formation of GR_{SO_4} with $y = 3$ from the reaction of soluble Fe^{2+} with ferrihydrite (poorly ordered ferric hydroxide). Thus, the activity of Fe^{3+} of reaction 1 was assumed to be controlled by the solubility of ferrihydrite (reaction 2)

$$Fe_4^{II}Fe_2^{III}(OH)_{12}SO_4{\cdot}yH_2O \rightleftharpoons 4Fe^{2+}_{(aq)} + 2Fe^{3+}_{(aq)} + 12OH^-_{(aq)} + SO^{2-}_{4(aq)} + yH_2O \quad (1)$$

$$Fe^{3+}_{(aq)} + 3OH^-_{(aq)} \rightleftharpoons Fe(OH)_{3(s)} \quad (2)$$

However, this assumption leads to imprecise estimation of $\Delta_fG^o(GR_{SO_4})$ because the variability of the solubility of ferrihydrite depends on its chemical composition (Majzlan *et al*., 2004). The value for $\Delta_fG^o(GR_{SO_4})$ was determined by Refait *et al*. (1999) by measuring simultaneous values of pH and electrochemical potential (E_h) in aqueous suspensions where freshly precipitated $Fe(OH)_2$ was oxidized to form GR_{SO_4}:

$$6Fe(OH)_{2(s)} + SO^{2-}_{4(aq)} \rightleftharpoons Fe_4^{II}Fe_2^{III}(OH)_{12}SO_{4(s)} + 2e^- \quad (3)$$

Those authors assumed that reaction 3 proceeded under equilibrium conditions and estimated $\Delta_fG^o(GR_{SO_4})$ by applying the Nernst equation as follows:

$$E_h(r) = \left[\frac{\Delta G_f^\circ(GR_{SO_4(s)}) - \Delta G_f^\circ(SO^{2-}_{4(aq)}) - 6\Delta G_f^\circ(Fe(OH)_{2(s)})}{2\times 96485}\right] - 0.029\log a(SO_4^{2-}) \quad (4)$$

where $E_h(r)$ refers to the redox potential of the reaction and $a(SO_4^{2-})$ denotes the activity of SO_4^{2-}. This electrochemical approach gave a value of $\Delta_fG^o(GR_{SO_4})$ of -3790 ± 10 kJ mol^{-1}. This value differs significantly from the value found by Hansen *et al*. (1994). The difference between the two estimates may be attributed to: (1) the inaccurate assumption used by Hansen *et al*. (1994) in which the activity of $Fe^{3+}_{(aq)}$ was controlled by the solubility of ferrihydrite; (2) the potential error (non-reversibility, mixed potentials) which may originate from using redox measurements in non-acid Fe^{II}-Fe^{III} systems; (3) the use of different sets of thermodynamic data where Refait *et al*. (1999) used values given by Kelsall and Williams (1991), while Hansen *et al*. (1994) used the dataset gathered by Wagman *et al*. (1982); and (4) the use of different synthetic routes to obtain GR_{SO_4}.

Discrepancies in experimental thermodynamic data of a specific Fe hydroxide/oxide have been observed many times (*e.g.* Cornell and Schwertmann, 2003). These discrepancies also exist when similar approaches (*i.e.* electrochemical, calorimetric, or equilibrium measurements) are used to calculate the thermodynamic data (Patrick and Thompson, 1953). These discrepancies are due to several factors, including physical parameters of the solids, purity, crystallinity, particle size, and specific characteristics of the experimental setups, *e.g.* purity of solutions and type of electrodes used (Devidal *et al*., 1996; Patrick and Thompson, 1953). Validating and complementing existing thermodynamic data by experiments using other approaches is, therefore, important.

The aim of this work was to estimate the $\Delta_fG^o(GR_{SO_4})$ from experimental data obtained during acid dissolution of GR_{SO_4} at 25ºC.

EXPERIMENTAL

All chemicals were of analytical grade and triple deionized water (20 MOhm cm^{-1}, Millipore, USA) was used throughout. The synthesis, redispersion of GR_{SO_4}, and all reactions were carried out under an Ar atmosphere (99.9995%).

Synthesis of GR_{SO_4}

GR_{SO_4}, $Fe_4^{II}Fe_2^{III}(OH)_{12}SO_4{\cdot}yH_2O$, was synthesized according to the procedure described by Koch and Hansen (1997). The procedure comprises controlled partial aerial oxidation of $FeSO_4$ solutions at constant pH 7.00. By this method, stoichiometric GR_{SO_4} is formed. The stoichiometry and properties of the GR_{SO_4} thus obtained have been reported elsewhere (Erbs *et al*., 1999; Hansen *et al*., 1996; Koch and Hansen, 1997).

Titration experiments

Freshly precipitated GR_{SO_4} was filtered and washed with deionized water. The GR_{SO_4} was suspended in 160 mL of 0.1 M Na_2SO_4 and equilibrated for 60–90 min. 80 mL of this suspension was transferred to 100 mL glass-infusion bottles fitted with a rubber septum. One glass-infusion bottle was used for each titration experiment. The titration was carried out by coupling an automatic dispensing unit (DOSIMAT 665) and a pH glass electrode (No. 6.0.0255.110), both supplied by Metrohm (Herisau, Switzerland), to glass-infusion bottles through the rubber septum. The GR suspensions (initial $[GR_{SO_4}] \approx 3.5$ mM, initial ionic strength $\approx 0.256\pm0.002$ M) were titrated slowly using 1 M H_2SO_4 as the titrant, and the titrations were stopped when the pH of the system was $\leqslant 3.00$. The system was stirred constantly (680 rpm) and protected from light by wrapping in aluminum foil. A constant temperature (25 ± 1ºC) was maintained with a water jacket connected to a Hetofrig water bath coupled with a Hetotherm thermostat, both supplied by Heto (Denmark). A constant gas flow of Ar (78 mL min^{-1}) was maintained in order to ensure anoxic conditions in the system.

In total, eight syntheses and titration experiments were carried out: T01–T08 (Table 1). For titrations T01–T06, the total aqueous concentrations of Fe^{II} were determined at different time intervals during the titration, while pH values were recorded at time intervals listed in Table 1. Powder X-ray diffraction (XRD) analyses of the products were carried out at the end of the titrations. The remaining two titrations, T07 and T08, were dedicated to phase analysis using Mössbauer spectroscopy and XRD analysis, and the concentrations

https://doi.org/10.1346/CCMN.2008.0560604 Published online by Cambridge University Press

Table 1. Parameters for titration of GR_{SO_4} with 1 M H_2SO_4 as well as the average crystallite thickness (*c* axis[a]) of the starting GR_{SO_4} at 25ºC.

Experiment	Initial pH	Titrant dose (mL)[b]	Equilibration time (min)[c]	Titration rate (mL min^{-1})	Initial GR_{SO_4} (XRD) crystallite size (nm)
T01	8.43	0.002	5	4.0×10^{-4}	36
T02	8.19	0.002	10	2.0×10^{-4}	40
T03	8.13	0.002	15	1.3×10^{-4}	44
T04	8.09	0.002	15	1.3×10^{-4}	44
T05	8.16	0.002	15	1.3×10^{-4}	44
T06	8.29	0.002	15	1.3×10^{-4}	45
T07[d]	8.10	0.002	15	1.3×10^{-4}	n.d.
T08[d]	8.16	0.002	15	1.3×10^{-4}	47

[a] Calculated from 003 basal reflections and using the Scherrer equation.
[b] Experimental error: ±25%.
[c] Time interval used for the system to reach a constant pH.
[d] Experiments used for characterization of solid phases formed during the titrations.
n.d.: Not determined

of Fe^{II} were determined at the beginning and at the end of the titrations.

Analyses

The amount of Fe^{II} present in solution, Fe^{II}_{sol}, and the total amount of Fe^{II} in the titration systems, Fe^{II}_{tot}, was determined by sampling 2 mL of GR suspensions from the reaction mixtures using a 5 mL, Ar-flushed polyethylene syringe. One mL of the suspension was treated for 30 min with 20 mL of 6 M HCl to dissolve GR and other solid species and 1 mL of this solution was used to determine Fe^{II}_{tot}. The remaining 1 mL was passed through a 0.22 μm Millipore filter and the filtrate was used to determine Fe^{II}_{sol}. The determinations were performed in duplicate. The Fe^{II} concentration was quantified by a modified phenanthroline method (Fadrus and Maly, 1975).

X-ray diffraction was performed using a Siemens D5000 X-ray diffractometer and CoKα radiation, in conjunction with a diffracted-beam monochromator. Samples for XRD were prepared by collecting the solids on a 0.22 μm Millipore filter. Glycerol was added in order to protect the filtered samples from oxidation, as described by Hansen (1989). The glycerol paste was smeared onto glass plates and scanned at a rate of 1º2θ min^{-1} over the range 5–80º2θ.

The Mössbauer absorbers were prepared by filtration of 4 mL aliquots through a 0.22 μm Millipore filter. Then, the solids collected together with the filter membrane were placed into Perspex capsules, which were immediately dropped into liquid N_2 and stored at this temperature until analysis. Mössbauer spectra were obtained at 250 K (and some at 180 and 150 K) using a constant acceleration spectrometer and a ^{57}Co source in Rh. The isomer shifts are given relative to the centroid of the room temperature spectrum of α-Fe. The spectra were fitted using a simple Lorentzian line shape and the relative absorption areas were assumed to be identical to relative abundance in the sample. Following previous work, the spectrum of GR_{SO_4} was fitted using two components (Koch, 1998).

Computational methods

The activities of SO_4^{2-}, H_2O, and Fe^{2+} ions were calculated at 25ºC using the geochemical software *PHREEQC* version 2 for Windows (Parkhurst and Appelo, 1999). The Davies equation was used to estimate the activity coefficients.

THERMODYNAMIC CALCULATIONS

Preliminary experiments showed that the slow acid titration of GR_{SO_4} suspended in 0.1 M Na_2SO_4, using 1 M H_2SO_4 as the titrant, produced magnetite, Fe_3O_4, according to the following equation:

$$Fe^{II}_4Fe^{III}_2(OH)_{12}SO_4{\cdot}yH_2O + 4H^+_{(aq)} \rightleftharpoons Fe_3O_{4(s)} + 3Fe^{2+}_{(aq)} + (y+8)H_2O_{(l)} + SO^{2-}_{4(aq)} \quad (5)$$

where, y is the number of water molecules present in the structure of GR_{SO_4}. Until recently, no precise determinations of y had been available, but GR_{SO_4} with $y = 8$ has been reported (Simon *et al*., 2003). In the present work, y was not estimated for the initial GR_{SO_4}, due to the lack of a precise and reliable technique for the determination of the water content in GR. However, irrespective of the amount of water present in the structure of GR, the non-oxidative dissolution of GR_{SO_4} will consume H^+ to form Fe^{2+} in a stoichiometric ratio between consumed H^+ and Fe^{2+} released equal to 0.75 (reaction 5). The reaction quotient (Q) of reaction 5 is defined as:

$$Q = \left[\frac{a(Fe^{2+})^3 \cdot a(H_2O)^{(y+8)} \cdot a(SO_4^{2-})}{a(H^+)^4}\right] \quad (6)$$

https://doi.org/10.1346/CCMN.2008.0560604 Published online by Cambridge University Press

Table 2. Experimental stoichiometric ratios, calculated logarithms of the reaction quotients (log Q), and Gibbs energies ($\Delta_r G^o$) of the acid-titration experiments at 25ºC[a].

Experiment	$-[Fe^{2+}]_{released} = m[H^+]_{consumed}-$ m	r^2	n[b]	I[c] (M)	Log Q	$\Delta_r G^o$ (kJ mol^{-1})[d]
T01	0.7377±0.0135	0.9993	4	0.267±	18.29±0.06	−104.40±0.35
T02	0.7070±0.0232	0.9926	4	0.266±	18.33±0.24	−104.64±1.38
T03	0.7070±0.0074	0.9986	5	0.269±	17.81±0.32	−102.22±1.43
T04	0.7567±0.0097	0.9995	5	0.267±	18.20±0.23	−103.82±1.50
T05	0.7142±0.0270	0.9972	4	0.268±	18.36±0.22	−104.82±1.24
T06	0.7491±0.0257	0.9965	4	0.269±	18.33±0.29	−104.60±1.64
Average	–	–	–	–	18.22±0.10	−104.08±0.55

[a] Within reaction zone A (see Figure 1 and equation 6 for definitions).
[b] Number of data points.
[c] Average ionic strength.
[d] Calculated using equation 7.

where, $a(X)$ refers to the activity of the element or compound X. Due to the great ionic strength of the reaction solutions (Table 2), the activity of water was slightly <1 ($a(H_2O)$ = 0.9950±0.0001 M, n: 49, average value including all the titrations) and therefore it is included in Q. At equilibrium, Q is equal to the equilibrium constant of reaction, K_r, and thus the standard Gibbs energy of reaction 5, $\Delta_r G^o$, can be estimated using equation 7:

$$\Delta_r G^o = -RT\ln K_r \quad (7)$$

where, R and T refer to the gas constant and the absolute temperature, respectively. Depending on the hydration of GR_{SO_4}, two types of $\Delta_r G^o$ can be distinguished: $\Delta_r G^o$(hydrated) and $\Delta_r G^o$(anhydrous) which refer to the standard Gibbs energy of reaction 5 when hydrated and anhydrous GR_{SO_4} are used, respectively. When $\Delta_f G^o$(products) of reaction 5 are known (Table 3), $\Delta_f G^o$(hydrated GR_{SO_4}) and $\Delta_f G^o$(anhydrous GR_{SO_4}) can be calculated from equations 8 and 9:

$$\Delta_f G^o(\text{hydrated } GR_{SO_{4(s)}}) = [\Delta_f G^o(Fe_3O_{4(s)}) + 3\Delta_f G^o(Fe^{2+}_{(aq)}) + (y + 8)\Delta_f G^o(H_2O_{(l)}) + \Delta_f G^o(SO^{2-}_{4(aq)})] - \Delta_r G^o(\text{hydrated}) \quad (8)$$

$$\Delta_f G^o(\text{anhydrous } GR_{SO_{4(s)}}) = [\Delta_f G^o(Fe_3O_{4(s)}) + 3\Delta_f G^o(Fe^{2+}_{(aq)}) + 8\Delta_f G^o(H_2O_{(l)}) + \Delta_f G^o(SO^{2-}_{4(aq)})] - \Delta_r G^o(\text{anhydrous}) \quad (9)$$

Because we have not been able to obtain a precise value of y for the starting GR_{SO_4}, the final figure for $\Delta_f G^o$(hydrated GR_{SO_4}), calculated according to equation 8, awaits a reliable measurement of y. However, y is considered a constant for GR_{SO_4} synthesized using the present method.

A common assumption in the calculation of $\Delta_f G^o$ of minerals is to consider the mineral in its anhydrous form and then add the hydration energy in order to obtain $\Delta_f G^o$ of the hydrated mineral (Tardy *et al.*, 1992). Applied to GR_{SO_4} this gives:

Table 3. Standard Gibbs energies of formation, $\Delta_f G^o$, at 25ºC.

Species	$\Delta_f G^o$ (kJ mol^{-1}) Robie and Hemingway (1995)	Majzlan *et al.* (2003)
Iron species:		
$Fe^{2+}_{(aq)}$	−90.00±2.0	–
$Fe^{3+}_{(aq)}$	−16.7±2.0	–
$Fe_3O_{4(s)}$	−1012.70±2.1	–
Lepidocrocite, γ-$FeOOH_{(s)}$	–	−480.1±1.4
Goethite, α-$FeOOH_{(s)}$	–	−489.8±1.2
Maghemite, γ-$Fe_2O_{3(s)}$	–	−727.9±2.0
Other species:		
$SO^{2-}_{4(aq)}$	−744.00±0.4	–
$H_2O_{(l)}$	−237.10±0.1	–
$OH^-_{(aq)}$	−157.3±0.1	–

https://doi.org/10.1346/CCMN.2008.0560604 Published online by Cambridge University Press

$$\Delta_f G^o(\text{hydrated } GR_{SO_{4(s)}}) = \Delta_f G^o(\text{anhydrous } GR_{SO_{4(s)}}) + \Delta G^o(\text{hyd}) + y \times \Delta_f G^o(H_2O) \quad (10)$$

where ΔG^o(hyd) refers to the standard Gibbs energy of hydration of anhydrous GR_{SO_4}. By combining equations 8, 9, and 10, we obtain:

$$\Delta_r G^o(\text{hydrated}) = \Delta_r G^o(\text{anhydrous}) - \Delta G^o(\text{hyd}) \quad (11)$$

According to equation 11, $\Delta_r G^o$(hydrated) and $\Delta_r G^o$(anhydrous) differ by a factor equal to ΔG^o(hyd) of the starting GR_{SO_4}. Studies on ΔG^o(hyd) for clay phyllosilicates gave values from −21 to −88 kJ/mol depending on variables such as particle size, the nature of the interlayer cation, layer charge, and the composition of the layers (Tardy and Duplay, 1992). Unfortunately, the ΔG^o(hyd) value for GR_{SO_4} has never been determined, so its contribution to $\Delta_r G^o$(hydrated) is unknown, but ΔG^o(hyd) probably has a similar magnitude to that seen for phyllosilicates. Thus, the assumption that $\Delta_r G^o$(hydrated) = $\Delta_r G^o$(anhydrous) is clearly imprecise and should not be used.

Apart from reaction 5, GR can also transform to magnetite *via* its oxidation by oxygen (reaction 12). Thus, for the consistency of our thermodynamic calculations, the formation of magnetite under strict anoxic conditions is important, *i.e.* exclusively *via* reaction 5. Monitoring the concentration of Fe^{II}_{tot} over time is one way to ascertain that parallel GR oxidation has not taken place, as Fe^{II} will be consumed during the oxidation of GR and not only redistributed as in reaction 5.

$$Fe^{II}_4Fe^{III}_2(OH)_{12}SO_4{\cdot}yH_2O + O_{2(g)} \rightleftharpoons Fe_3O_{4(s)} + (y+6)H_2O_{(l)} + SO^{2-}_{4(aq)} + 2H^+_{(aq)} \quad (12)$$

RESULTS

A typical titration curve (Figure 1) has two distinct regions: an initial plateau (zone A and B) with an almost constant pH: 7.40±0.14, n = 1407 (average for all the titration experiments), followed by zone C, which is characterized by a sharp decline in pH and a later progressive stabilization of pH at ~3. Magnetite and goethite were identified by XRD as the mixed end products of the titrations under anoxic conditions to pH 3.00 (data not shown).

The titration curves can be divided into three different zones, A, B, and C, according to their ratio: $[Fe^{2+}]_{released}/[H^+]_{consumed}$. The plots of $[Fe^{2+}]_{released}$ *vs.* $[H^+]_{consumed}$ corresponding to each titration experiment (Figure 2) show that the measured data are distributed among different zones, corresponding to lines of different slopes. In all the titrations, the data distributed between the beginning of the titration until the point at which 0.25 mL of titrant (zone A) was added, resulted in stoichiometric $[Fe^{2+}]_{released}/[H^+]_{consumed}$ ratios of 0.75, as predicted by reaction 5 (Table 2). This result suggests that magnetite is the only solid product at this stage. The data measured at later stages of the titrations, after zone A to the end of the titration, can be fitted by straight lines with slopes which are <<0.75; this indicates that another reaction, in addition to reaction 5, is taking place. Examination of the final products of reaction revealed that goethite apparently was formed.

The identity of the products formed at the end of zone A was probed for titrations T07 and T08 by XRD (Figure 3). The analyses showed the presence of unreacted crystalline GR_{SO_4} and magnetite produced during the titration. The XRD patterns of both starting

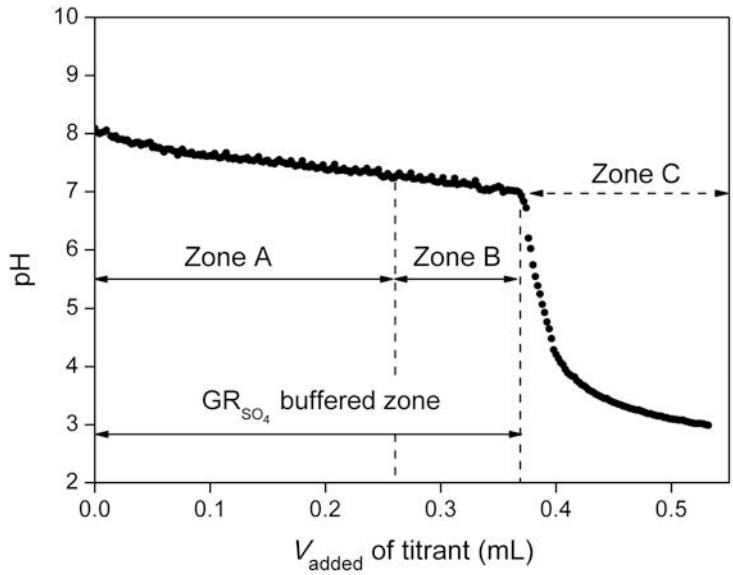

Figure 1. Example of a titration curve (T04). For definitions of zones A, B, and C, see text.

https://doi.org/10.1346/CCMN.2008.0560604 Published online by Cambridge University Press

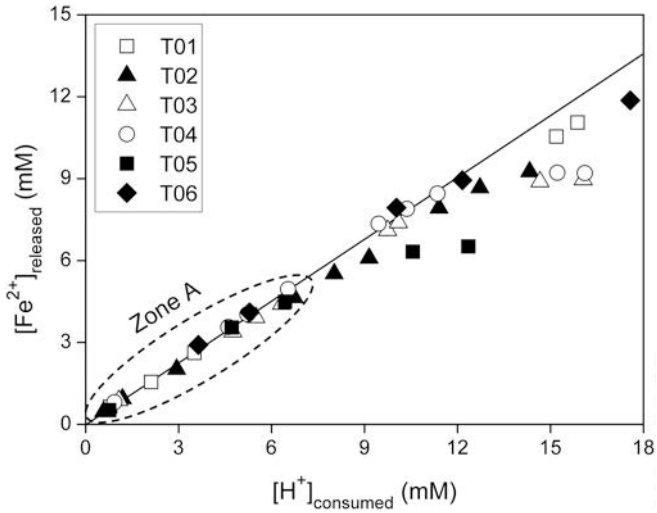

Figure 2. Relationship between the concentrations of Fe^{2+} released into solution, $[Fe^{2+}]_{released}$, and H^+ consumed, $[H^+]_{consumed}$, at zone A. The solid line represents the ideal stoichiometric ratio with slope 0.75.

and remaining GR_{SO_4} consisted of symmetrical and sharp peaks (full width at half maximum: 0.32±0.04º2θ and 0.26±0.04º2θ, respectively). These features are characteristic of high crystallinity. A slight decrease in the width of the diffraction peaks was observed at the end of zone A (data not shown), which may be due to some preferential dissolution of the small GR particles, ageing of the GR particles (Ostwald ripening) and/or variation between measurements. The basal spacing was calculated from the reflections as $d = ([d_{003} + 2 \times d_{006} + 3 \times d_{009}]/3)$.

Mössbauer spectra measured at 250 K of the reaction mixture samples at the end of zone A reveal two doublets and two sextets (Figure 4) and the hyperfine parameters of these components are summarized in Table 4 together with reference values of GR_{SO_4} and magnetite. Mössbauer spectra were also measured at 180 and 150 K and analyses of these data give similar results to the spectra at 250 K. This indicates the absence of Fe-bearing phases other than GR and magnetite. The spectra at 250 K exhibits two doublets corresponding to Fe^{II} and Fe^{III} of the GR_{SO_4} and two sextets attributed to the A and

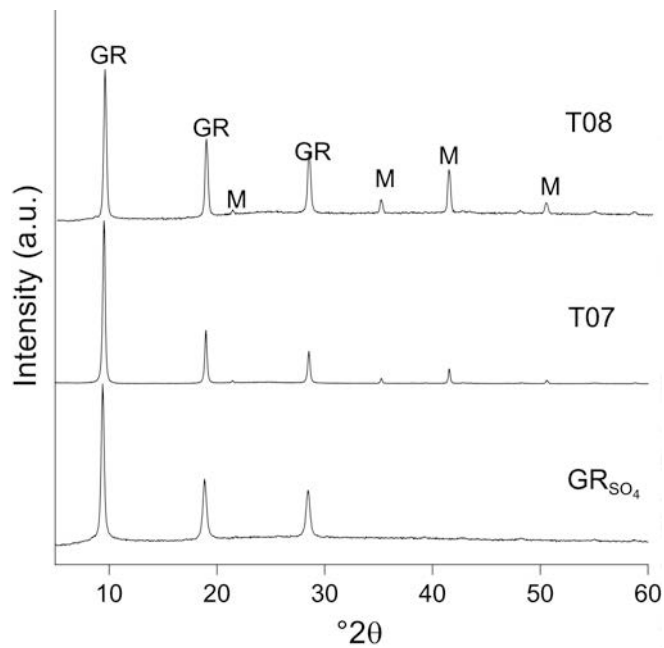

Figure 3. XRD patterns of the solids in the reaction mixture formed at the initial zone A for GR_{SO_4} in experiments T07 and T08, at 25ºC, and of synthesized GR_{SO_4}. GR: green rust sulfate, M: magnetite.

https://doi.org/10.1346/CCMN.2008.0560604 Published online by Cambridge University Press

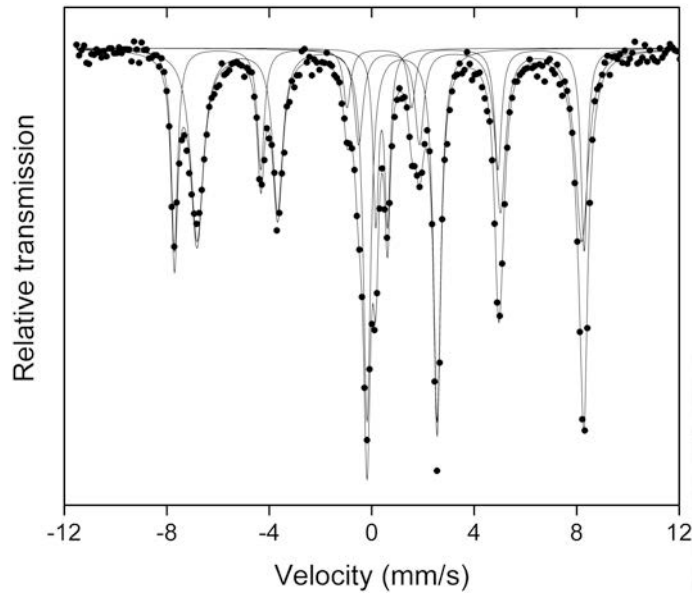

Figure 4. Mössbauer spectrum measured at 250 K of the sample obtained following zone A from titration T07. Dots are experimental points and solid lines are fit components and the sum of the components.

B sites of magnetite (Table 4). The hyperfine parameters of the remaining GR_{SO_4} do not differ significantly from the characteristic parameters of pure GR_{SO_4}. Although the relative area of the two components due to Fe^{II}/Fe^{III} in the remaining GR deviates from the initial value of 2, the lines of the doublets are narrow and their relative intensities are similar. The ratios between areas of the two sextets B and A are different from 2, indicating the non-stoichiometric nature of the magnetite formed (Häggström *et al*., 1978). B/A ratios different from 2 are also found for mixtures of magnetite and maghemite but the small line widths of the octahedral and tetrahedral sites observed in the Mössbauer spectra (Table 4) indicates the presence of a single phase. This

Table 4. Mössbauer hyperfine parameters of GR_{SO_4} and magnetite (Fe_3O_4) from two experiments measured at 250 K. Reference values for components in pure GR_{SO_4} and a natural sample of magnetite are included.

Experiment	Species	Components	B_{hf}[a] (Tesla)	δ[b] (mm s^{-1})	ΔE_Q (ε)[c] (mm s^{-1})	Γ[d] (mm s^{-1})	RA[e] (%)
T07	GR_{so_4}	Fe^{2+}	–	1.17(2)	2.69(2)	0.38(2)	32.6(6)
		Fe^{3+}	–	0.40(4)	0.44(4)	0.27(3)	10.5(7)
	Fe_3O_4	A	48.9(5)	0.30(3)	0.00(3)	0.37(3)	20.6(7)
		B	46.0(5)	0.68(3)	0.01(3)	0.61(5)	36.4(7)
T08	GR_{SO_4}	Fe^{2+}	–	1.18(3)	2.74(3)	0.35(3)	24.6(7)
		Fe^{3+}	–	0.37(5)	0.46(5)	0.26(4)	8.3(9)
	Fe_3O_4	A	49.6(5)	0.30(4)	0.00(4)	0.29(3)	22.9(7)
		B	46.6(5)	0.68(4)	0.01(4)	0.60(6)	44.2(7)
	GR_{SO_4}[f]	Fe^{2+}	–	1.21(2)	2.70(2)	0.29(2)	66.0(5)
		Fe^{3+}	–	0.41(2)	0.47(2)	0.28(2)	33.0(5)
	Fe_3O_4[g]	A	49.0(2)	0.27(2)	0.01(2)	0.36(2)	30.0(5)
		B	45.8(2)	0.66(2)	0.00(2)	0.47(2)	61.0(5)

[a] B_{hf}: magnetic hyperfine field.
[b] δ: isomer shift relative to α-iron.
[c] ΔE_Q: quadrupole splitting of doublet; ε: quadrupole shift of sextet.
[d] Γ: full width at half maximum.
[e] RA: Relative area of components.
[f] GR_{SO_4} was synthesized in the authors' laboratory.
[g] Natural sample of magnetite measured at 298 K and contains 9% Fe in silicates.
Values in parenthesis are estimated uncertainties on the last digit.

https://doi.org/10.1346/CCMN.2008.0560604 Published online by Cambridge University Press

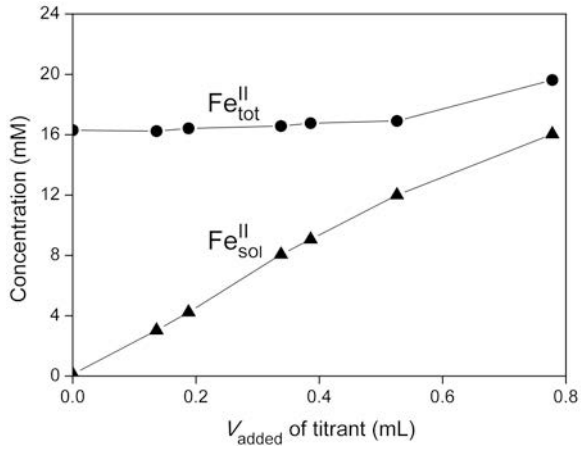

Figure 5. Monitoring of the concentrations of total Fe^{II} (Fe^{II}_{tot}) and aqueous Fe^{II} (Fe^{II}_{sol}) along the time span of titration T06 to assess stability of anoxic conditions.

leads to the conclusion that maghemite is not formed in the titration experiments, in agreement with determinations of Fe^{II} during the experiment.

The change in Fe^{II}_{tot} was measured through all titration experiments to document maintenance of anoxic conditions (Figure 5). The behavior of Fe^{II}_{tot} *vs.* time was the same for all the titrations: the concentration was kept constant until ~0.5 mL of the titrant was added (zones A, B, and beginning of C). At the end of the titration an increase in Fe^{II}_{tot} was observed, which was probably due to evaporation processes caused by sampling and/or the constant flux of Ar applied to the reaction flasks. Since no decrease in the concentration of Fe^{II}_{tot} was observed during the titrations, and in particular in zone A, the leakage of oxygen into the systems and thus parallel GR oxidation reactions could be disregarded.

Because the activity of water in all the titrations was very close to unity ($a(H_2O)$ = 0.9950±0.0001, n = 49, average value including all the titrations), the effect of y on the value of log Q was found to be less than experimental error (data not shown, equation 6). In order to evaluate equilibrium conditions, the log Q values of the titration experiments were plotted *vs.* the volume of titrant added (Figure 6). As can be seen in Figure 6, log Q is constant at the beginning of the titrations, specifically in the region with $[Fe^{2+}]_{released}/[H^+]_{consumed}$ ratios close to 0.75, zone A (Table 2). The invariability of log Q is a strong indication of chemical equilibrium. Thus, the inference is that the reaction quotient actually represents the equilibrium constant of reaction 5, K_r, and therefore $\Delta_r G^o$ can be calculated using the data corresponding to zone A (Table 2).

DISCUSSION

The buffered regions observed at the beginning of the titration curves (zones A and B) are due to consumption of the H^+ added when GR_{SO_4} dissolves with the simultaneous precipitation of magnetite and release of Fe^{II}. At equilibrium, the increase in the aqueous concentration of Fe^{II} is followed by an increase in the concentration of H^+ (see equation 6) and thus a decrease in pH, which explains the gently descending slope in zones A and B. Zone C starts when GR_{SO_4} has completely dissolved and therefore the addition of further H^+ causes a sharp decrease in pH.

Magnetite and goethite (α-FeOOH) were identified as the end products of the titrations. However, the ratio close to 0.75 found at the initial stages of the titration (zone A) fits with the theoretical relationship expected for the exclusive formation of magnetite, which was confirmed by XRD and Mössbauer spectroscopy

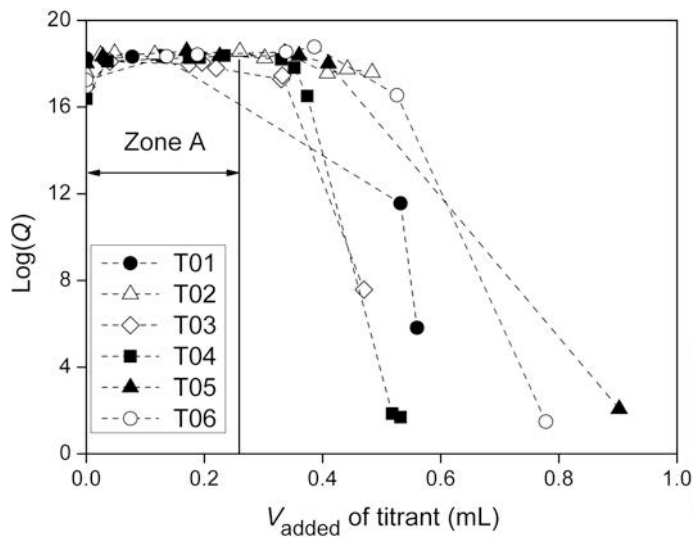

Figure 6. Change of the logarithm of the reaction quotients, log (Q), *vs.* the extent of titration.

https://doi.org/10.1346/CCMN.2008.0560604 Published online by Cambridge University Press

(Figures 3, 4). Both XRD and Mössbauer analysis show the existence of two solid phases at these stages: GR_{SO_4} and non-stoichiometric magnetite. The narrow and symmetric diffraction peaks of the remaining GR_{SO_4} demonstrate its high crystallinity. Also, the similarity with the initial GR_{SO_4} is indicated by similarity of parameters and narrow line widths.

Stoichiometric magnetite has the structural formula: $[Fe^{III}]_A[Fe^{III}Fe^{II}]_BO_4$, where A and B refer to the tetrahedral and octahedral interstitial sites, respectively, of a face-centered cubic arrangement formed by the oxygen ions. Non-stoichiometric magnetite, $[Fe^{III}]_A[Fe^{III}_{1+2x}Fe^{II}_{(1-3x)}\square_x]_BO_4$ with $0 < x < 0.33$ and $\square$ representing cationic vacancies, is formed due to vacancies or cationic impurities at the interstitial sites (Daniels and Rosencwaig, 1969). The oxidation of Fe^{II} in the magnetite may be one of the reasons for the existence of these vacancies. However, this does not apply to our experiments because leakage of oxygen into our systems did not occur and only chemicals of high purity were used. Hence, the reaction mechanism by which GR_{SO_4} dissolves is the most likely cause of the formation of non-stoichiometric magnetite in the present systems.

The transformation of GR_{SO_4} into non-stoichiometric magnetite *via* acid dissolution can be written in a more general way as:

$$Fe^{II}_4Fe^{III}_2(OH)_{12}SO_4{\cdot}yH_2O + 4\left(\tfrac{1+3x}{1+x}\right)H^+ \rightleftharpoons \left(\tfrac{1}{1+x}\right)Fe^{III}_{2(1+x)}Fe^{II}_{1-3x)}\square_x]O_4 + \left(\tfrac{3+7x}{1+x}\right)Fe^{2+} + \left(\tfrac{8+12x}{1+x}+y\right)H_2O_{(l)} + SO_4^{2-} \quad (13)$$

with $0 < x < 0.33$, and where y and $\square$ represent the molecules of structural water and the cationic vacancies, respectively. The limits of the reaction are reached when $x = 0$ and when $x = 0.33$, which corresponds to the formation of stoichiometric magnetite, Fe_3O_4, and maghemite, γ-Fe_2O_3, respectively. From equation 13, the stoichiometric ratio $[Fe^{2+}]_{released}/[H^+]_{consumed}$ can be predicted in the whole range of x; and reciprocally, x can be estimated from experimental $[Fe^{2+}]_{released}/[H^+]_{consumed}$ ratios. The x values calculated from our experimental ratios (Table 3) are summarized in Table 5; according to the estimated x values, the stoichiometry of the magnetite formed at the end of zone A varies in the different titrations. In other words, the magnetite formed ranged from highly non-stoichiometric (T02–T03) to stoichiometric (T06). However, the variation in terms of stoichiometry seems to have a negligible effect on the Δ_rG^o of the acid dissolution of GR_{SO_4}, as can be seen from the small error related to the average value of Δ_rG^o (Table 2). The effect associated with the non-stoichiometry of magnetite on Δ_rG^o is considered to be less than experimental error. Hence, the use of reaction 5, in which the formation of stoichiometric magnetite is assumed, to calculate $\Delta_fG^o(GR_{SO_4})$ can be considered a good approximation.

Table 5. Chemical formulae of magnetite at the end of reaction zone A.

Experiment	x^a	Formula of magnetite
T01	0.027±0.001	$[Fe^{III}_{2.05}Fe^{II}_{0.92}\square_{0.03}]O_4$
T02	0.116±0.005	$[Fe^{III}_{2.23}Fe^{II}_{0.65}\square_{0.12}]O_4$
T03	0.116±0.002	$[Fe^{III}_{2.23}Fe^{II}_{0.65}\square_{0.12}]O_4$
T04	−0.013±0.000	$[Fe^{III}_{1.97}Fe^{II}_{1.03}]O_4$
T05	0.091±0.005	$[Fe^{III}_{2.18}Fe^{II}_{0.73}\square_{0.09}]O_4$
T06	0.002±0.000	$[Fe^{III}_{2.00}Fe^{II}_{1.00}]O_4$

[a] Calculated using equation 13.

Gibbs standard energy of formation of GR_{SO_4}

In order to obtain a reliable value for $\Delta_fG^o(GR_{SO_4})$, the use of accurate, reliable, and consistent thermodynamic data for each of the reactants and products involved in equation 8 is necessary. Initially, three well known thermodynamic datasets were considered as potential datasets to be used in the calculations: Wagman *et al*. (1982), Bard *et al*. (1985), and Robie and Hemingway (1995). The only significant differences in Δ_fG^o between sources were found for $Fe^{2+}_{(aq)}$ and $Fe_3O_{4(s)}$. $\Delta_fG^o(Fe^{2+}_{(aq)})$ from Wagman *et al*. (1982) is more positive ($\Delta_fG^o(Fe^{2+}_{(aq)}) = 78.9$ kJ mol^{-1}) than the values given in the other databases. The value adopted by this dataset was taken from electrochemical data and hence some of the discrepancies have been attributed to the differences in the preparation of the electrodes, which were used in the electrochemical cells, as well as the presence of small amounts of oxygen contamination (Tremaine and Leblanc, 1980; Parker and Khodakovskii, 1995). A wide set of $\Delta_fG^o(Fe^{2+}_{(aq)})$ values, obtained using different methods until 1982, was reviewed by Parker and Khodakvskii (1995), who recommended the value of −90.53±1.0 kJ mol^{-1}. This value is consistent with the value given by Robie and Hemingway (1995, Table 3).

The identity of the magnetite where stoichiometry and purity were used to determine $\Delta_fG^o(Fe_3O_4)$ in Wagman *et al*. (1982) and Bard *et al*. (1985) is unknown, because no clear reference is made to original data in either case. This is not the case for the $\Delta_fG^o(Fe_3O_4)$ value given by Robie and Hemingway (1995), in which the value was taken from Hemingway *et al*. (1990), who recalculated heat capacities for pure and stoichiometric synthetic magnetite at different temperatures. In conclusion, because the thermodynamic data compiled by Robie and Hemingway (1995) were evaluated critically and documented fully, they were used for both the solid and solution phases. Additional Δ_fG^o values, not found in the work by Robie and Hemingway (1995) (*e.g.* lepidocrocite, goethite and maghemite), were taken from Majzlan *et al*. (2003) (see Table 3).

https://doi.org/10.1346/CCMN.2008.0560604 Published online by Cambridge University Press

Table 6. Standard Gibbs energy of formation of GR_{SO_4} and the corresponding solubility products at 25ºC.

Reference	$\Delta_f G^o$ (kJ mol^{-1})	log K_{sp} [b]
This study	−3819.4±6.44	−139.2±4.8
Refait *et al.* (1999)	−3790±10	−134.0±5.9
Hansen *et al.* (1994)[c]	−3668.7±4.0	−112.8±4.3

[a] GR form without considering the molecules of intercalated water: $Fe^{II}_4Fe^{III}_2(OH)_{12}SO_4$.
[b] Calculated using reaction 1 and with the number of water molecules equals to zero except for our value.
[c] Recalculated from the hydrated form of GR_{SO_4} ($Fe^{II}_4Fe^{III}_2(OH)_{12}SO_4{\cdot}3H_2O$) by subtracting $3 \times \Delta_f G^o(H_2O)$.

The combination of equation 8, the average measured $\Delta_r G^o$ (Table 2), and $\Delta_f G^o$ values listed in Table 3 permits the deduction of a mathematical expression in which $\Delta_f G^o$ of GR_{SO_4} with '*y* water molecules' can be calculated at 25ºC:

$$\Delta_f G^o(Fe^{II}_4Fe^{III}_2(OH)_{12}SO_4{\cdot}yH_2O) = -3819.43(\pm 6.44) + y{\cdot}[\Delta_f G^o(H_2O_{(l)})] \quad (14)$$

Comparisons with previously reported ΔG^o_f (GR_{SO_4}) values

Previously reported $\Delta_f G^o$ values, as well as their respective solubility products, K_{sp}, for GR_{SO_4} are listed in Table 6. All values refer to the hydrated forms but do not mention the contribution of the interlayer water in the absolute value for $\Delta_f G^o(GR_{SO_4})$ as precise estimates of *y* had not been obtained. The value of $\Delta_f G^o(GR_{SO_4})$ determined in the present work is more negative than the previously reported $\Delta_f G^o$ values (Table 6). The discrepancies may be caused by using different GR values containing different amounts of interlayer water which hence affect the $\Delta_r G$ values. In addition, differences in the structural order of the GR_{SO_4}, caused by the different synthesis methods used, as well as the different treatment of the GR_{SO_4} after synthesis and during the experiments, may also contribute to the observed differences. For example, Refait *et al.* (1999) determined $\Delta_f G^o$ from freshly precipitated GR_{SO_4}, and the chemical analyses were mostly carried out in the same system in which the GR_{SO_4} was precipitated. In contrast, in the present study, the GR_{SO_4} was separated from the synthesis solution and washed before suspension in 0.1 M $NaSO_4$.

GR redox reactions

Common products of the oxidation of GR are goethite (α-FeOOH), lepidocrocite (γ-FeOOH), maghemite (γ-Fe_2O_3), and magnetite, Fe_3O_4 (Taylor, 1980; Erbs *et al.*, 1999; Benali *et al.*, 2001). The formation of a specific end product is determined by the rate of oxidation, temperature, pH, solution composition, and other parameters. The reduction potentials for half cells involving GR_{SO_4} at standard conditions as well as in aqueous solution at pH = 7 and $a(SO_4^{2-}) = 10^{-3}$ were calculated using equation 14. The half cell with the smallest reduction potential is the GR_{SO_4}-magnetite couple.

Table 7. Reduction potentials of some redox couples involving GR_{SO_4} at 25ºC.

Half reactions	E^o (V)	E (V)[a]	Reference
Green rust sulfate:			
$6H^+ + SO_4^{2-} + 6\gamma\text{-FeOOH} + 4e^- \rightleftharpoons Fe^{II}_4Fe^{III}_2(OH)_{12}SO_4$	0.50	−0.16	This study
$6H^+ + SO_4^{2-} + 3H_2O + 3\gamma\text{-}Fe_2O_3 + 4e^- \rightleftharpoons Fe^{II}_4Fe^{III}_2(OH)_{12}SO_4$	0.47	−0.20	This study
$6H^+ + SO_4^{2-} + 6\alpha\text{-FeOOH} + 4e^- \rightleftharpoons Fe^{II}_4Fe^{III}_2(OH)_{12}SO_4$	0.35	−0.31	This study
$4H^+ + SO_4^{2-} + 4H_2O + 2Fe_3O_4 + 2e^- \rightleftharpoons Fe^{II}_4Fe^{III}_2(OH)_{12}SO_4$	0.53	−0.39	This study
Others:			
$NO_3^- + 10H^+ + 8e^- \rightleftharpoons NH_4^+ + 3H_2O$	0.88	0.37	Stumm and Morgan (1996)
$HCrO_4^- + 7H^+ + 3e^- \rightleftharpoons Cr^{3+} + 3H_2O$	1.20	0.23	Morel and Hering (1993)
$CrO_4^{2-} + 8H^+ + 3e^- \rightleftharpoons Cr^{3+} + 3H_2O$	1.07	−0.03	Morel and Hering (1993)
$HAsO_4^{2-} + 3H^+ + 2e^- \rightleftharpoons H_2AsO_3^- + H_2O$	0.58	−0.04	Sadiq (1997)
$HAsO_4^{2-} + 2H^+ + 2e^- \rightleftharpoons HAsO_3^{2-} + H_2O$	0.21	−0.20	Sadiq (1997)

[a] Values calculated at pH = 7 with the activities of oxidized and reduced species equal to 1, except for the activities of Cr- and As-species and sulfate which were = 10^{-3}.

https://doi.org/10.1346/CCMN.2008.0560604 Published online by Cambridge University Press

Some other important environmental redox couples (Table 7) confirm that the reduction of relevant environmental species such as chromate (CrO_4^{2-}) and nitrate (NO_3^-) by GR_{SO_4} is thermodynamically feasible; while the reduction of As(V) as the oxyanion $HAsO_4^{2-}$ is less favorable, though still possible. This thermodynamic factor, together with kinetic factors, may be the reason why GR_{SO_4} cannot reduce As(V) to As(III) (Randall *et al*., 2001).

CONCLUSIONS

In this study, $\Delta_f G^o(GR_{SO_4})$ was determined by equilibrium measurements of the acidic dissolution of GR_{SO_4} at room temperature to form magnetite. The analysis of the changes in the reaction quotients of the acid dissolution of GR_{SO_4} demonstrated that GR_{SO_4} dissolves under equilibrium conditions and thus from these experiments the equilibrium constant for the dissolution process can be determined. The absolute value of $\Delta_f G^o(GR_{SO_4})$ depends on the amount of interlayer water, y, and it can be given as:

$$-3819.43\pm6.44 \text{ kJ mol}^{-1} + y \times [\Delta_f G^o(H_2O_{(l)})]$$

The new value for $\Delta_f G^o(GR_{SO_4})$ led to a solubility product, log K_{sp}, of 139.2 ± 4.8. Similarly the redox potentials of several half cells involving anhydrous GR_{SO_4} were estimated and compared. The most reducing half cell in aqueous neutral media with sulfate activity of 10^{-3} is the GR_{SO_4}-magnetite couple with a reduction potential of −0.39 V.

ACKNOWLEDGMENTS

The authors are grateful to Hanne Nancke-Krogh for carrying out some of the chemical analyses.

REFERENCES

Bard, A.J., Parsons, R., and Jordan, J. (1985) *Standard Potentials in Aqueous Solution*. Marcel Dekker Inc., New York, 848 pp.

Benali, O., Abdelmoula, M., Refait, P., and Genin, J.M.R. (2001) Effect of orthophosphate on the oxidation products of Fe(II)-Fe(III) hydroxycarbonate: The transformation of green rust to ferrihydrite. *Geochimica et Cosmochimica Acta* **65**, 1715–1726.

Bernal, J.D., Dasgupta, D.R., and Mackay, A.L. (1959) The oxides and hydroxides of iron and their structural interrelationships. *Clay Minerals Bulletin* **4**, 15–64.

Bourrie, G., Trolard, F., Genin, J.M.R., Jaffrezic, A., Maitre, V., and Abdelmoula, M. (1999) Iron control by equilibria between hydroxy-Green Rusts and solutions in hydromorphic soils. *Geochimica et Cosmochimica Acta* **63**, 3417–3427.

Cornell, R.M. and Schwertmann, R.M. (2003) *The Iron Oxides: Structure, Properties, Reactions, Occurrences and Uses*. Wiley-VCH, Weinheim, Germany, 664 pp.

Daniels, J.M. and Rosencwaig, A. (1969) Mössbauer spectroscopy of stoichiometric and non-stoichiometric magnetite. *Journal of Physics and Chemistry of Solids*, **30**, 1561–1571.

Devidal, J.L., Dandurand, J.L., and Gout, R. (1996) Gibbs free energy of formation of kaolinite from solubility measurement in basic solution between 60 and 170ºC. *Geochimica et Cosmochimica Acta*, **60**, 553–564.

Erbs, M., Hansen, H.C.B., and Olsen, C.E. (1999) Reductive dechlorination of carbon tetrachloride using iron(II) iron(III) hydroxide sulfate (green rust). *Environmental Science and Technology* **33**, 307–311.

Fadrus, H. and Maly, J. (1975) Suppression of iron(III) interference in determination of iron(II) in water by 1,10-phenanthroline method. *Analyst* **100**, 549–554.

Furukawa, Y., Kim, J.W., Watkins, J., and Wilkin, R.T. (2002) Formation of ferrihydrite and associated iron corrosion products in permeable reactive barriers of zero-valent iron. *Environmental Science and Technology* **36**, 5469–5475.

Genin, J.M.R., Ruby, C., Gehin, A., and Refait, P. (2006) Synthesis of green rusts by oxidation of $Fe(OH)_2$, their products of oxidation and reduction of ferric oxyhydroxides; Eh-pH Pourbaix diagrams. *Comptes Rendus Geoscience*, **338**, 433–446.

Häggström, L., Annersten, H., Ericsson, T., Wappling, R., Karner, W., and Bjarman, S. (1978) Magnetic dipolar and electric quadrupolar effects on Mössbauer-spectra of magnetite above Verwey transition. *Hyperfine Interactions*, **5**, 201–214.

Hansen, H.C.B. (2001) Pp. 469–493 in: Environmental chemistry of iron(II)-iron(III) LDHs (Green rusts) in: *Layered Double Hydroxides: Present and Future* (V. Rives, editor). Nova Science Pub Inc., New York.

Hansen, H.C.B., Borggaard, O.K., and Sørensen, J. (1994) Evaluation of the free energy of formation of Fe(II)-Fe(III) hydroxy-sulphate (green rust) and its reduction of nitrite. *Geochimica et Cosmochimica Acta*, **58**, 2599–2608.

Hansen, H.C.B., Koch, C.B., Krogh, H.N., Borggaard, O.K., and Sørensen, J. (1996) Abiotic nitrate reduction to ammonium: key role of green rust. *Environmental Science and Technology*, **30**, 2053–2056.

Hemingway, B.S. (1990) Thermodynamic properties for bunsenite, NiO, magnetite, Fe_3O_4, and hematite, Fe_2O_3, with comments on selected oxygen buffer reactions. *American Mineralogist*, **75**, 781–790.

Kelsall, G.H. and Williams, R.A. (1991) Electrochemical-behavior of ferrosilicides (Fexsi) in neutral and alkaline aqueous-electrolytes. 1. Thermodynamics of Fe-Si-H_2O systems at 298 K. *Journal of the Electrochemical Society*, **138**, 931–940.

Koch, C.B. (1998) Structures and properties of anionic clay minerals. *Hyperfine Interactions*, **117**, 131–157.

Koch, C.B. and Hansen, H.C.B. (1997) Reduction of nitrate to ammonium by sulphate green rust. *Advances in GeoEcology* **30**, 373–393.

Legrand, L., El Figuigui, A., Mercier, F., and Hausse, A. (2004) Reduction of aqueous chromate by Fe(II)/Fe(III) carbonate green rust: kinetic and mechanistic studies. *Environmental Science and Technology*, **38**, 4587–4595.

Majzlan, J., Grevel, K.D., and Navrotsky, A. (2003) Thermodynamics of Fe oxides: Part II. Enthalpies of formation and relative stability of goethite (α-FeOOH), lepidocrocite (γ-FeOOH), and maghemite (γ-Fe_2O_3). *American Mineralogist*, **88**, 855–859.

Majzlan, J., Navrotsky, A., and Schwertmann, U. (2004) Thermodynamics of iron oxides: Part III. Enthalpies of formation and stability of ferrihydrite (~$Fe(OH)_3$), schwertmannite (~$FeO(OH)_{3/4}(SO_4)_{1/8}$), and ε-$Fe_2O_3$. *Geochimica et Cosmochimica Acta*, **68**, 1049–1059.

Morel, F.M.M. and Hering, J.G. (1993) *Principles and Applications of Aquatic Chemistry*. Wiley, New York, 588 pp.

Myneni, S.C.B., Tokunaga, T.K., and Brown, G.E. (1997) Abiotic selenium redox transformations in the presence of

Fe(II,III) oxides. *Science*, **278**, 1106–1109.
Parker, V.B. and Khodakovskii, I.L. (1995) Thermodynamic properties of the aqueous ions (2+ and 3+) of iron and the key compounds of iron. *Journal of Physical and Chemical Reference Data*, **24**, 1699–1745.
Parkhurst, D.L. and Appelo, C.A.J. (1999) User's guide to PHREEQC (version 2): A computer program for speciation, batch-reaction, one-dimensional transport and inverse geochemical calculations. Water-Resources Investigations, *U.S. Geological Survey* Report 99–4256. Denver, Colorado.
Patrick, W.A. and Thompson, W.E. (1953) Standard electrode potential of the iron ferrous ion couple at 25ºC. *Journal of the American Chemical Society*, **75**, 1184–1187.
Phillips, D.H., Watson, D.B., Roh, Y., and Gu, B. (2003) Mineralogical characteristics and transformations during long-term operation of a zerovalent iron reactive barrier. *Journal of Environmental Quality*, **32**, 2033–2045.
Randall, S.R., Sherman, D.M., and Ragnarsdottir, K.V. (2001) Sorption of As(V) on green rust ($Fe_4(II)Fe_2(III)(OH)_{12}SO_4 \cdot 3H_2O$) and lepidocrocite (γ-FeOOH): Surface complexes from EXAFS spectroscopy. *Geochimica et Cosmochimica Acta*, **65**, 1015–1023.
Refait, P., Bon, C., Simon, L., Bourrie, G., Trolard, F., Bessiere, J., and Genin, J.M.R. (1999) Chemical composition and Gibbs standard free energy of formation of Fe(II)-Fe(III) hydroxysulphate green rust and Fe(II) hydroxide. *Clay Minerals*, **34**, 499–510.
Robie, R.A. and Hemingway, B.S. (1995) Thermodynamic properties of minerals and related substances at 298.15 K and 1 Bar (10^5 pascals) pressure and at higher temperatures. *U.S. Geological Survey Bulletin*, **1452**, 461 pp.
Rodriguez, J.J.S. and Gonzalez, J.E.G. (2006) Identification and formation of green rust 2 as an atmospheric corrosion product of carbon steel in marine atmospheres. *Materials and Corrosion-Werkstoffe und Korrosion*, **57**, 411–417.
Sadiq, M. (1997) Arsenic chemistry in soils: An overview of thermodynamic predictions and field observations. *Water, Air and Soil Pollution*, **93**, 117–136.
Simon, L., Francois, M., Refait, P., Renaudin, G., Lelaurain, M., and Génin, J.R. (2003) Structure of the Fe(II-III) layered double hydroxysulphate green rust two from Rietveld analysis. *Solid State Sciences*, **5**, 327–334.
Stumm, W. and Morgan, J.J. (1996) *Aquatic Chemistry. Chemical Equilibria and Rates in Natural Waters*. Wiley, New York, 1022 pp.
Taylor, R.M. (1980) Formation and properties of Fe(II)Fe(III) hydroxy-carbonate and its possible significance in soil formation. *Clay Minerals*, **15**, 369–382.
Tardy, Y. and Duplay, J. (1992) A method of estimating the Gibbs free-energies of formation of hydrated and dehydrated clay-minerals. *Geochimica et Cosmochimica Acta*, **56**, 3007–3029.
Tremaine, P.R. and Leblanc, J.C. (1980) The solubility of magnetite and the hydrolysis and oxidation of Fe^{2+} in water to 300ºC. *Journal of Solution Chemistry*, **9**, 415–442.
Wagman, D.D., Evans, W.H., Parker, V.B., Schumm, R.H., Halow, I., Bailey, S.M., Churney, K.L., and Nuttall, R.L. (1982) The NBS tables of chemical thermodynamic properties – selected values for inorganic and C-1 and C-2 organic-substances in SI Units. *Journal of Physical and Chemical Reference Data*, vol. **11**, supplement 2.

(*Received 20 December 2007; revised 15 August 2008; Ms. 0108*; A.E. J.D. Fabris)